Journal of Solid State Chemistry 183 (2010) 1484–1489

Contents lists available at ScienceDirect

Journal of Solid State Chemistry

journal homepage: www.elsevier.com/locate/jssc

# New bismuth calcium oxysilicate with apatite structure: Synthesis and structural characterization

Vladimir Uvarov [a,*], Sanaa Shenawi-Khalil [b], Inna Popov [a]

[a] The Unit for Nanoscopic Characterization, The Center for Nanoscience and Nanotechnology, The Hebrew University of Jerusalem, Jerusalem 91904, Israel
[b] Casali Institute of Applied Chemistry, The Institute of Chemistry, The Hebrew University of Jerusalem, Jerusalem 91904, Israel

ARTICLE INFO

*Article history:*
Received 26 January 2010
Received in revised form
29 March 2010
Accepted 5 April 2010
Available online 28 April 2010

*Keywords:*
Apatite structure
Bismuth calcium oxysilicate
Powder X-ray diffraction
$HSiO_4$ group
Charge compensation
Isomorphous substitutions

ABSTRACT

New bismuth calcium silicon oxide $Ca_4Bi_{4.3}(SiO_4)(HSiO_4)_5O_{0.95}$, with apatite structure has been synthesized. The structure was refined from powder X-ray diffraction data. The refinement revealed that the phase has $P6_3/m$ (176) space group with unit cell parameters $a=b=9.6090(7)$ Å, $c=7.0521(7)$ Å, $V=563.9$ Å$^3$ and $c/a=0.734$. The $R_{wp}$ factor at Rietveld refinement was equal to 0.082. The synthesized phase has an unusual quantity of cation vacancies in a crystal lattice. Mechanisms of compensation of the excess charge of a lattice are considered and checked experimentally using the FT-IR spectroscopy, the thermal analysis and the XPS analysis.



## 1. Introduction

The apatite structure is a common type of atomic packing occurring in various natural and synthetic compounds. The generalized chemical formula of isostructural apatite phases can be written as $M_{10-x}(TO_4)_6A_{2y}$, where $M$ is a one or a few large cations ($K^{1+}$, $Na^{1+}$, $Ca^{2+}$, $Ba^{2+}$, $Sr^{2+}$, $La^{3+}$, $Ce^{3+}$, $Bi^{3+}$, etc.), $TO_4$ is an anionic group ($PO_4^{3-}$,$VO_4^{3-}$ ,$SiO_4^{4-}$, etc.) and $A$ is an anion ($F^-$,$OH^-$, $O^{2-}$, $S^{2-}$, etc.). $PO_4^{3-}$ is the most widespread anionic group in the minerals with apatite structure. However, synthetic phases exhibited greater variety of chemical composition. For example $Ca_2La_8(SiO_4)_6O_2$ [1], $Pr_9K(SiO_4)_6O_2$ [2], $CaLa_3Bi_2(SiO_4)_3O$ [3], $Ca_2Ce_8(SiO_4)_6O_2$ [4], $NaLa_9(GeO_4)_6O_2$ [5], $BiCa_4(VO_4)_3O$ [6] and other phases with apatite structure have been synthesized. The majority of phases with apatite structure are crystallized in $P6_3/m$ (57%), $P6_3$ (21%) and $P-3$ (9%) space groups [7]. The space group of an ideal apatite structure is $P6_3/m$ (176). Within this structure large cations occupy two non-equivalent 4*f* and 6*h* crystallographic sites. It is commonly accepted that a prediction of their precise positioning on these two sites is impossible [1], although trivalent cations are known to have a tendency to occupy a 6*h* site. Usually the value of $x$ in the generalized apatite chemical formula is close to 0. Nakayama et al. [8] had synthesized a new type of oxide ionic conductors belonging to a series $La_{10-x}(SiO_4)_6O_{3-y}$ ($La$=La, Nd, Sm, Gd, Dy, etc.) with $x=0\div6$. The synthesized phases preserved the apatite structure at $x\leq4$. Authors [8] reported a tetragonal structure instead of the hexagonal apatite structure in compounds with high cation deficiency ($x=4\div6$). But, the issue of excess lattice charge and its compensation was not considered in this work. In this paper we report on the synthesis and the structural characterization of a new bismuth calcium oxysilicate belonging to apatite-type crystalline compounds with unusually high cation deficiency.

## 2. Experimental

### 2.1. Synthesis

Stoichiometric amounts of $Ca(NO_3)_2\cdot4H_2O$ and $Bi(NO_3)_3\cdot5H_2O$ (Fisher Chemical) were mixed under sonication with appropriate amounts of ethanol and nitric acid to form transparent colorless solution. Certain amount of mesoporous silica KIT-6 dry sample was added to the solution. Then the mixture was heated to dryness over a 12 h period at 80 °C. The final product was obtained by calcination of dried material at 800 °C (5 °C/min) for 12 h and silica framework was etched with a 2 M NaOH aqueous solution. It was whitish fine crystallite powder with negligible quantity of dark orange particles.

* Corresponding author.
*E-mail address:* vladimiru@savion.huji.ac.il (V. Uvarov).

0022-4596/$ - see front matter © 2010 Elsevier Inc. All rights reserved.
doi:10.1016/j.jssc.2010.04.028

### 2.2. Structural characterization

Crystalline structure of the specimens was analyzed by powder X-ray diffraction. Measurements were performed on D8 Advance diffractometer (Bruker AXS, Karlsruhe, Germany) with a goniometer radius 217.5 mm, Göbel Mirror parallel-beam optics, 2° Sollers slits and 0.6 mm receiving slit. Low background quartz sample holder was carefully filled with the powder samples. The XRD patterns from 5 to 85° $2\theta$ were recorded at room temperature using Cu$K\alpha$ radiation ($\lambda$=0.15418 nm) with the following measurement conditions: tube voltage of 40 kV, tube current of 40 mA, step scan mode with a step size 0.02° $2\theta$ and counting time of 1 s per step for preliminary study and 12 s per step for structural refinement. TOPAS-v.3 [9] software was used for structure refinement and structure presentation. Pseudo-Voigt function was used as a profile function for the Rietveld refinement.

FT-IR spectra were acquired with ALPHA-P Module (Bruker Optics Gmbh) with diamond ATR object. Morphological observations and identification of chemical composition were performed with environmental scanning electron microscope (ESEM) Quanta 200 (FEI Company, Netherland) equipped with the EDS detector (EDAX-TSL, USA). Chemical bonding of atoms composing the tested material was studied by the X-ray photoelectron spectroscopy (XPS) using the Kratos XPS Axis Ultra spectrometer. For the thermogravimetric analysis (TGA) Mettler TC10A/TC15 TA controller and Mettler M3 thermobalance (Greifensee, Switzerland) were used. Samples of 20–25 mg were weighed and heated to 25–700 °C at a rate of 2 °C/min.

## 3. Results and discussion

Careful examination of an XRD pattern obtained from a powder specimen reveals that the specimen contains several crystalline phases. Indexing of this XRD pattern showed that the major component of the tested material is a hexagonal phase with unit cell parameters $a=b\approx 9.61$ Å and $c\approx 7.05$ Å. Analysis of the intensity distribution and extinctions over the diffraction peaks clearly indicate that the major phase has an apatite structure with space group $P6_3/m$ or $P6_3$. More precise identification of the space group is impossible, since extinction rules are identical for $P6_3/m$ or $P6_3$. According to the EDS analysis (see Fig. 1), the as-synthesize sample contains Bi, Ca, Si and O. Based on this elemental composition and on the XRD data, we performed thorough search within the commonly accepted informational recourses (PDF, FizNIST, MinCrys, etc) and concluded that the main phase of the tested samples is a new unknown phase. However, later we found the only publication (Engel et al. [10]), in which chemical compound described as ($Ca_{3.2}Bi_{6.8}(SiO_4)_6O_{1.4}$) had been reported yet without structural solution. Authors [10] noted that they had not received comprehensible values of $R$ factors in the course of structure refinement. Namely, they obtained (i) the $R$ factor value of 22% for the model in which all Bi atoms occupy 6$h$ site and (ii) the $R$ factor of 38% for a statistical distribution of Bi atoms over 4$f$ and 6$h$ sites.

Additional phases observed in the experimental XRD pattern were identified as eulytite ($Bi_4(SiO_4)_3$, PDF-33-215) and wollastonite ($CaSiO_3$, PDF-84-0655). Presence of additional phases within as-synthesized samples of $M_{10-x}(TO_4)_6A_{2-y}$ type materials was reported by a number of authors ($La_2SiO_5$[8], $Bi_3(SiO_4)_3$ [10], $Nd_2SiO_5$[11] ) and is known to occur even when stoichiometric amounts of components are used for synthesis. Formation of these phases possibly can be considered as an intrinsic property of the process of synthesis of apatite-type phases in which bivalent cations heterogeneously substitute those of trivalent cations. From this point of view, the chemical formula of the newly synthesized apatite phase should be written as $Ca^{2+}_{x1}Bi^{3+}_{x2}(SiO^{4-}_4)_6O^{2-}_y(OH)^-_z$, i.e. to enter $(OH)^-$ in anion group. Variables $x1$, $x2$, $y$ and $z$ have to satisfy the following conditions: $6\le(x1+x2)\le 10$, $0\le y\le 2$ and $0\le z\le 2$. It should also be noted that the impurity of the same phases was observed by Engel et al. [10]. In addition, we observed very weak and wide hump of an amorphous material around 15–18° 2θ. Therefore, we estimated the content of apatite phases as 90–95%. This estimation was corroborated by the results of optical and scanning electron microscopic observations (see Supplementary materials). The crystallite size of the major phase calculated using the Scherrer's equation was about 80 nm.

The most important step preceding the Rietveld refinement is a choice of a structural model. The following considerations have been taken into account:

1. According to the EDS results obtained for different particles of a major phase, (Ca+Bi)/Si value is equal to 1.29–1.41 (mean value is 1.38) and Ca/Bi value is equal to 0.91–0.98 (mean value is 0.93). Hence the possible chemical formula of our phase can be written as $Ca_4Bi_{4.3}(SiO_4)_6O_y(OH)_z$. The phase with very similar low metal/silicon ratio was revealed by Quintas et al. [12] in calcium neodymium silicates with apatite structure. Authors assumed that this phase has wollastonite-type crystalline structure. Large amount of cation vacancies is known, but it is relatively a rare phenomenon. Additionally, in our case we deal with heterovalent substitution of $Bi^{3+}$ for $Ca^{2+}$ that requires balancing the excessive negative charge of crystalline lattice. The problem could be solved through a partial substitution of oxygen atoms in $[SiO_4]^{4-}$ tetrahedron and/or on 2$a$ site with hydroxyl ion $(OH)^-$. First substitution is known to occur, for example, in natural silicates [13,23,29–31]. Recently Dordevic et al. [14] reported observation of similar substitution mechanism in arsenate with apatite structure. They inferred the existence of $H^+$ outside the channel in oxyhydroxyapatites and provided possible atomic co-ordinates for a H atom in $HAsO^{2-}_4$. Get'man et al. [15] studied the possibility of isomorphous substitutions of $Eu^{3+}$ for $Sr^{2+}$ ($Sr^{2+}+OH^{1-}\rightarrow Eu^{3+}+O^{2-}$) in strontium hydroxovanadates and have shown that such replacement is possible within a wide range of Eu/Sr ratios. Formation of $HSiO_4$ groups in apatite structure was studied by Astala et al. [16] and Arcos et al. [17]. According to these authors, formation of $HSiO_4$ groups provides charge compensation in an apatite structure. That is why we suggested that the new phase may contain hydroxyl ions $(OH)^-$ as well, and thus it could be described as $Ca_4Bi_{4.3}(SiO_4)_{6-x}(HSiO_4)_xO_y(OH)_z$. Obviously that $(OH)^-$ hydroxyl ion should replace O(3) oxygen atom on 12$i$ site in $SiO_4$ tetrahedrons. A tentative 12$i$ site occupancy will be therefore $0.5O^{2-}/0.5(OH)^-$ approximately.
The correctness of our hypothesis was first checked using the FT-IR spectroscopy. The FT-IR spectrum obtained from the tested material is shown in Fig. 2. The IR absorption due to tetrahedral $SiO_4$ units can be assigned based on absorption bands at wavenumbers between 1100 and 800 $cm^{-1}$ (symmetric and antisymmetric stretching) and on relatively sharp bands at wavenumbers between 600 and 400 $cm^{-1}$ (symmetric and antisymmetric bending vibrations) [3,18]. These bands confirm the presence of orthosilicate group into the tested material. Presence of OH groups (Si–OH bonds) in $SiO_4$ tetrahedrons was confirmed by the absorption bands observed at 549.9, 815.5, 895.4 and 1093.2 $cm^{-1}$. The band at 549.9 $cm^{-1}$ is assigned to bending vibrations of Si–OH bonds [19] and the band at 815.5 $cm^{-1}$ is attributed to Si–OH

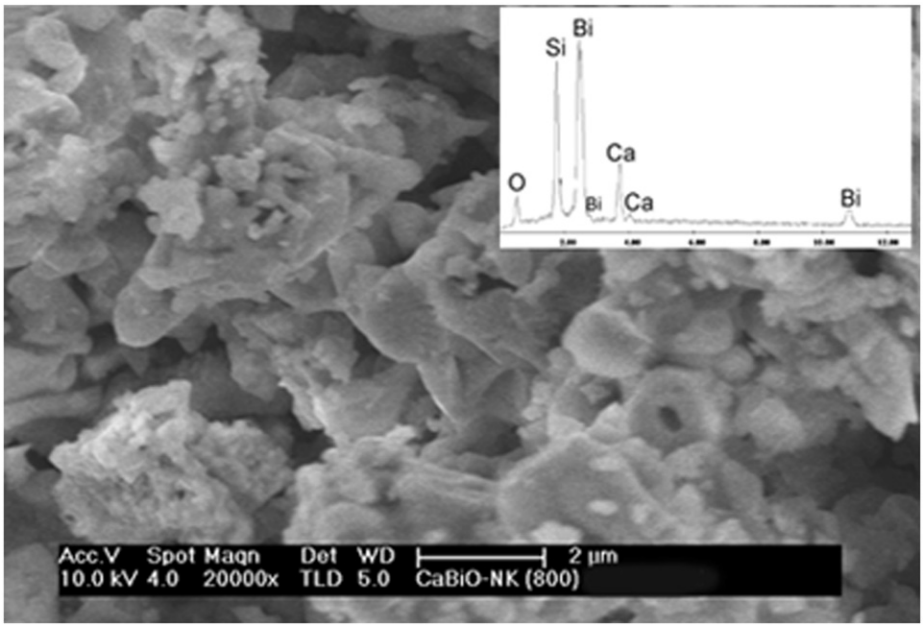


**Fig. 1.** SEM image and EDS spectrum (inset) obtained from synthesized phase.

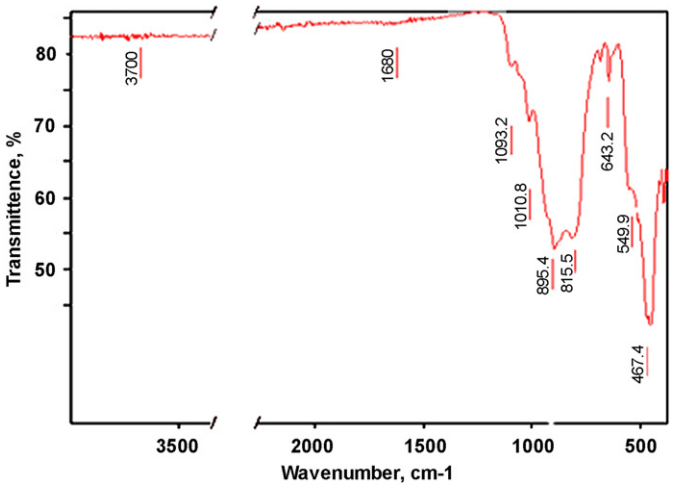


**Fig. 2.** FT-IR spectrum of synthesized phase.

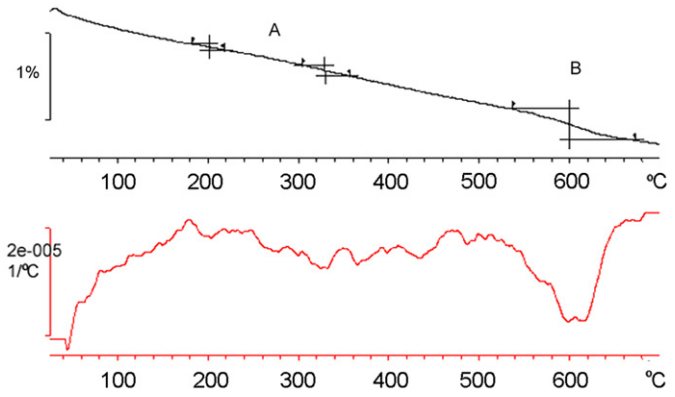


**Fig. 3.** Results of thermal analysis of the synthesized material. Upper and lower curves represent TGA and the first derivative of TGA curve, respectively.

bending in $SiO_4$ [17,20,21]. The band at 895.4 $cm^{-1}$ corresponds to symmetric stretching of all four Si–O bonds of $O_3SiOH$ with slight motion of a Si in the direction of the hydroxyl [17,22] and the band at 1093.2 $cm^{-1}$ is attributed to the $\delta$-OH vibration type of the Si–OH groups [23]. Appearance of these absorption bands is very important in our case as the experimental result confirming the correctness of the proposed structural model.

TGA curves obtained for the synthesized material are shown on Fig. 3. According to TGA, mass losses were observed in the interval 180–350 °C and at 600 °C. The first process could be attributed to desorption of water from powder material being exposed to open air and also could be correlated with a pre-dehydration process, while the second one could be related to dehydroxylation [24] resulted in total mass loss of about 0.56% (0.19% and 0.37% accordingly). The first derivative of TGA curve exhibited very weak peak at 600 °C. Similarly to Kendrick et al. [25], we explain this process as a replacement of OH groups in $HSiO_4$ tetrahedrons by oxygen.

2. It should be noted that the lattice charges within our phase could be balanced also if we suggest that a part of bismuth atoms in the unit cell has actual valence +5. Such possibility is mentioned by Engel et al. [10]. We used the XPS analysis to check the oxidation states of Bi and O atoms in the tested sample. These results are shown in Fig. 4. We found no evidence for $Bi^{5+}$ in the sample (see Fig. 4a). The photoelectron peak position 159.26 eV for Bi $4f_{7/2}$ perfectly matched that of a well-known $Bi^{3+}$ (159.3 eV) [26]. Simultaneously, we found that O 1*s* peak is composed of at least two major peaks appearing at 530.26 and 531.81 eV, respectively as shown in Fig. 4b. According to [27], the lower binding energy of 530.26 eV corresponds to oxygen within crystal structure while the higher one of 531.8 eV indicates the presence of hydroxyl groups. Thus XPS, FT-IR and thermal analysis confirm the presence of OH groups within the tested material. We suggest that the mesoporous silica KIT-6 used for synthesis may be considered as an intrinsic source for OH groups in structure of a new phase, although other precursors could contribute to proton supply as well. There is some probability that the detected OH groups relate to the residue of amorphous KIT-6 presenting in the sample. However, our

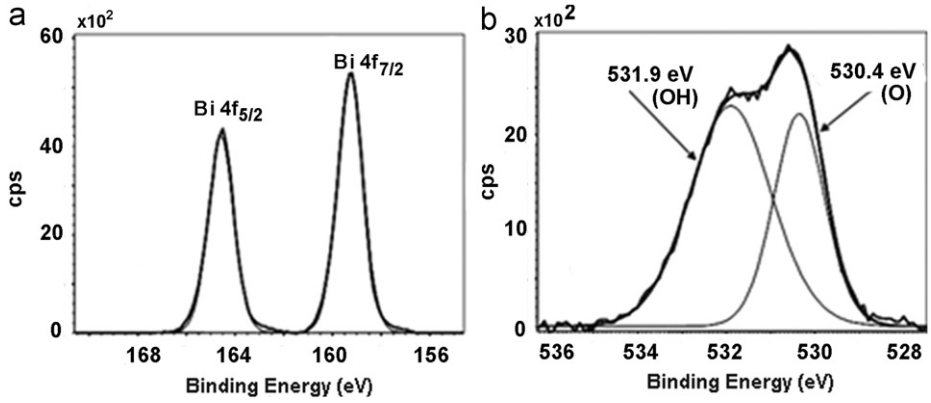


**Fig. 4.** Results of the XPS analysis: (a) photoelectron peak position for Bi and (b) photoelectron peak position for O1*s*.

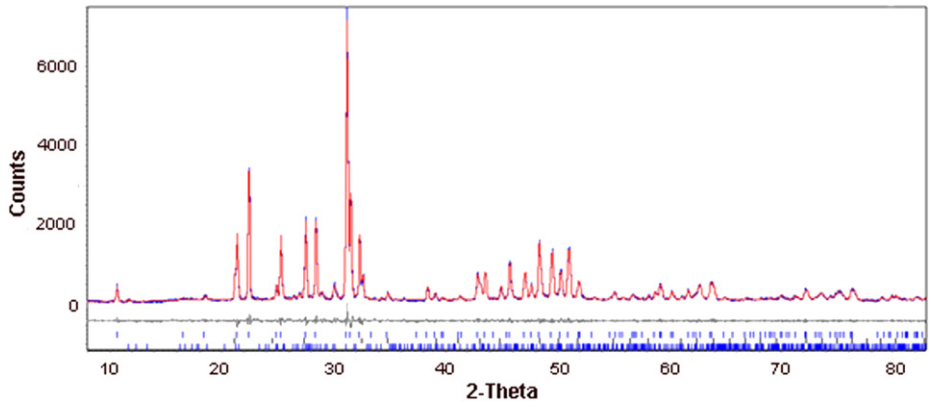


**Fig. 5.** Observed, calculated and difference X-ray diffraction profiles for the synthesized specimen. Positions of reflections are marked with vertical lines.

numerous previous analyses of a KIT-6 have not revealed the presence of OH groups in this material. In addition, the amount of an amorphous phase was insufficient and, in our opinion, cannot explain all the mass losses observed in TGA.

3. As an apatite-type structure is well-established, its geometrical bonding parameters (bond lengths, bond angles, geometry of cation and anion polyhedrons, etc.) are known for a number of chemical compounds. We used equations suggested by Mercier et al. [28] to construct a starting model for the Rietveld refinement. These equations relate atomic co-ordinates to unit cell parameters, bond lengths and angles and allow calculation of the atomic co-ordinates from the actual unit cell parameters and typical geometrical bonding parameters of the specific structural type.

The results of EDS, FT-IR, XPS and thermal analysis have been taken into account in the course of developing the initial model. When charge is balanced within the lattice through addition of OH groups, they could be localized either in $SiO_4$ tetrahedrons only or may also partially substitute oxygen atoms on a 2*a* site. We tested these two options under Rietveld refinement and found that the value of $R_{wp}$ factor was 2–3% higher for the latter one. Therefore, for a final refinement the first option for localization of OH groups was accepted. According to these considerations, final chemical formula $Ca_4Bi_{4.3}(SiO_4)(HSiO_4)_5O_{0.95}$ has been accepted. We have chosen $P6_3/m$ space group for a refinement although space group $P6_3$ has also been checked. We have received higher value of the $R_{wp}$ factor for this group, than for the $P6_3/m$ group. Co-ordinates of hydrogen atoms could not be extracted from conventional XRD data because of low scattering ability of hydrogen. Therefore, we excluded the positions of hydrogen atoms at the refinement. Site occupancy factors for Ca and Bi atoms were fixed to the chemical composition of the new phase. We considered ordered model and models with the mixed 4*f* and 6*h* site occupancies. It is very important that co-ordinates of atoms for models with the ordered and mixed site occupancies were the same. We ensured that chemical composition remained constant at occupancies refinement and coincided with the EDS results. Each of the refined parameter was accepted only if it was physically meaningful. The value of the site occupancy for the oxygen atom O(4) (not related to Si–O tetrahedron) is less than 1, but it is acceptable for apatite structure [17,29]. For example, Rosales et al. [29] reported on SOF=0.358 for O(4) atom in $Na_{2.27}Ho_{7.73}(SiO_4)_6O_{0.72}$. Co-ordinates of O(3) atom were "released" at a final stage of refinement. As a result we obtained 1.662 Å length for Si–OH bond. This value is in good agreement with the data reported by other authors for Si–OH bond lengths in crystalline phases with $HSiO_4$ tetrahedrons [30–32] and with the computed value of Si–OH bond length for an isolated $HSiO_4$ cluster that was obtained by Astala et al. [16]. Isotropic temperature factors (Beq) for sites with mixed occupancies

and for all oxygen atoms were fixed to Beq=2 at final refinement. We obtained $R_{wp}$=12.15% for the model with the ordered site occupancies, $R_{wp}$=16.6% for the model with the mixed 4*f* and 6*h* site occupancies and $R_{wp}$=8.22% for the model with the mixed 6*h* site occupancies. The results of Rietveld refinement for various models, table of bonds and angles and refinement report are presented in Supplementary materials.

The graphical result of structural refinement is shown in Fig. 5. Refined unit cell parameters are $a=b=9.6090(7)$ Å and $c=7.0521(7)$ Å. The $R_{wp}$ factor was equal to 8.22%. The final refined structural parameters and selected bond distances are given in Tables 1–3.

A fragment of $Ca_4Bi_{4.3}(SiO_4)(HSiO_4)_5O_{0.95}$ structure is shown in Fig. 6. One Si atom and four O atoms (or OH group) form tetrahedron. Si–O bond lengths vary from 1.61 to 1.63 Å. Since Si–OH bond length is equal to 1.662 Å, the tetrahedron containing OH group is slightly deformed. Ca atoms located on 4*h* sites form columnar polyhedrons and have 9-fold coordination with O atoms. Interatomic distances in these polyhedrons differ and are equal to 2.346 Å for Ca–O(1), 2.562 Å for Ca–O(2) and 2.767 Å for Ca–O(3). The important parameter, which is used for description of an apatite structure, is Ca metaprism twist angle $\varphi$. The size and the profile of tunnels depend on $\varphi$ value. Calculation of Ca metaprism twist angel $\varphi$ was performed using the formula suggested by White and ZhiLi [7]. We ascertain that $\varphi$ value for $Ca_4Bi_{4.3}(SiO_4)(HSiO_4)_5O_{0.95}$ is 16.4°. Silicon tetrahedrons and calcium polyhedrons have common oxygen atoms and thus are in contact (the so-called corner-connection). Bi atoms on 6*f* positions form two triangles, which are rotated 60° from each other around the *c*-axis. In the centre of these Bi-triangles, the oxygen atom O(4) (not related to Si–O tetrahedron) is located. Bond lengths and bond angles presented in the Tables 2 and 3 are in good agreement with the values reported by other authors [1–4,7,30–32].

**Table 1**
Crystallographic data for $Ca_4Bi_{4.3}(SiO_4)(HSiO_4)_5O_{0.95}$.

| Color | Off-white |
|---|---|
| *Empirical formula* | $Ca_4Bi_{4.3}(SiO_4)(HSiO_4)_5O_{0.95}$ |
| Crystal data: | |
| Crystal system | Hexagonal |
| Space group | $P6_3/m$ (176) |
| Lattice parameters (Å) | |
| $a=b$ | 9.6090(7) |
| $c$ | 7.0521(7) |
| Volume (Å$^3$) | 563.9(1) |
| Formula units | 1 |
| Density (g/cm$^3$) | 4.79 |
| *Structural refinement* | |
| Software | TOPAS v.3 |
| Profile function | Pseudo-Voigt |
| Parameters varied | 37 |
| $R_{exp}$ | 4.39 |
| $R_{wp}$ | 8.22 |
| $R_p$ | 4.53 |
| Goodness of fit | 1.87 |

## 4. Conclusion

New calcium bismuth oxysilicate with chemical composition $Ca_4Bi_{4.3}(SiO_4)(HSiO_4)_5O_{0.95}$ and apatite structure has been synthesized and its structure was refined using powder XRD data. Results of EDS, FT-IR, XPS and thermal analysis were used in the course of developing the initial model for Rietveld refinement of crystal structure. We suggested and confirmed experimentally

**Table 3**
Selected bond lengths (Å) and bond angles (°) for $Ca_4Bi_{4.3}(SiO_4)(HSiO_4)_5O_{0.95}$.

| | | | |
|---|---|---|---|
| *Bond length:* | | | |
| Ca–O1 | 2.342(62) | Bi-Si | 3.06(11) |
| Ca–O2 | 2.561(91) | Si-O1 | 1.63(15) |
| Ca–O3 | 2.766(43) | Si-O2 | 1.61(13) |
| Bi–O1 | 2.984(51) | Si-O3 | 1.662(72) |
| Bi–O2 | 2.267(58) | O1-O2 | 2.63(15) |
| Bi–O4 | 2.391(65) | O1-O3 | 2.718(90) |
| *Bond angles:* | | | |
| O1–Ca–O1 | 73.7(25) | O1-Si-O2 | 108.3(36) |
| O2–Ca–O2 | 74.4(33) | O1-Si-O3 | 111.3(40) |
| Bi–O3–Bi | 119.6(17) | O3-Si-O3 | 114.8(69) |

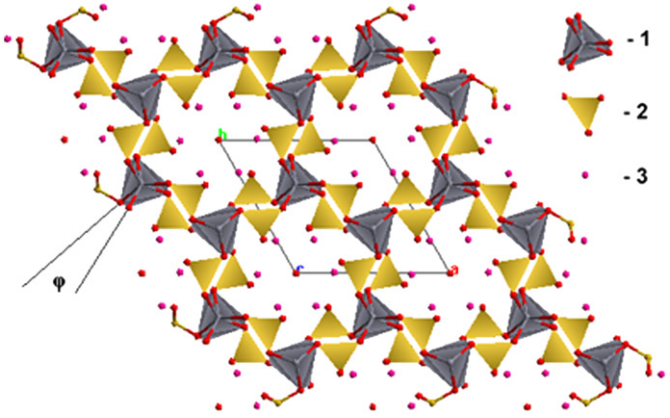


**Fig. 6.** The fragment $Ca_4Bi_{4.3}(SiO_4)(HSiO_4)_5O_{0.95}$ structure along *c*-axis in polygonal mode. Ca–O metaprisms (1) that form columnar polyhedrons corner-connected with $SiO_4$ tetrahedrons (2) and Bi atoms (3) that form Bi-triangles are represented. The hexagonal unit cell is shown.

**Table 2**
Refined atomic coordinates for $Ca_4Bi_{4.3}(SiO_4)(HSiO_4)_5O_{0.95}$.

| Site | Atom | *x* | *y* | *z* | Occ. | $B_{eq}$ (Å$^{-2}$) |
|---|---|---|---|---|---|---|
| Ca(4*f*) | $Ca^{2+}$ | 0.333 | 0.667 | 0.0100(41) | 0.574 | 0.75(9) |
| Bi(6*h*) | $Bi^{3+}/Ca^{2+}$ | 0.9920(22) | 0.2448(14) | 0.25 | 0.716/0.284 | 2 |
| Si(6*h*) | $Si^{4+}$ | 0.4049(66) | 0.3740(13) | 0.25 | 1 | 0.23(1) |
| O1(6*h*) | $O^{2-}$ | 0.3378(67) | 0.5000(81) | 0.25 | 1 | 2 |
| O2(6*h*) | $O^{2-}$ | 0.5990(15) | 0.4759(73) | 0.25 | 1 | 2 |
| O3(12*i*) | $O^{2-}$/OH | 0.3549(42) | 0.2665(54) | 0.0515(55) | 0.583/0.417 | 2 |
| O4(2*a*) | $O^2$ | 0 | 0 | 0.25 | 0.475(7) | 2 |

that lattice charge compensation was achieved through partial replacement of oxygen atoms into $SiO_4$ tetrahedrons by hydroxyl groups. The presence of OH group in structure (in $HSiO_4$ tetrahedron) is confirmed by results of the FT-IR spectroscopy, XPS and thermal analysis. Probably usage of mesoporous silica KIT-6 as a synthetic precursor provided easiness of oxygen/OH group replacement and thus it balances electric charge within a lattice of newly synthesized apatite phase. It was found that the phase has $P6_3/m$ (1 7 6) space group with unit cell parameters $a=b=9.6090(7)$ Å, $c=7.0521(7)$ Å, $V=563.9$ Å and $c/a=0.734$. The $R_{wp}$ factor was equal to 0.082.

Due to a high content of cation vacancies, we suppose that new $Ca_4Bi_{4.3}(SiO_4)(HSiO_4)_5O_{0.95}$ phase may exhibit unusual to this type of solids physical properties like enhanced ion conductivity and high luminescence, which can find practical applications.

Further details of the crystal structure investigation can be obtained from the Fachinformationszentrum Karlsruhe, 76344 Eggenstein-Leopoldshafen, Germany, (e-mail: crysdata@fiz.karlsruhe.de) on quoting the depository number CSD-420603.

## Acknowledgments

Authors wish to acknowledge Mr. Vitaly Gutkin for his assistance in the XPS analysis. Authors also thank the Unit for Nanocharacterization of the Harvery M. Krueger Center for Nanoscience and Nanotechnology at the Hebrew University of Jerusalem for the usage of its analytical equipment. S. Shenawi-Khalil thanks Pr.Y.Sasson for its support in the course of work.

## Appendix A. Supplementary material

Supplementary data associated with this article can be found in the online version at doi:10.1016/j.jssc.2010.04.028.

## References

[1] L.W. Schroeder, M. Mathew, Cation ordering in $Ca_2La_8(SiO_4)_6O_2$, J. Solid State Chem. 26 (1978) 383–387.
[2] F. Werner, F. Kubel, Apatite-type Pr9K(SiO4)6O2-a potential oxide ion conductor, Mater. Lett. 59 (2005) 3660–3665.
[3] N. Lakshminarasimhan, U.V. Varadaraju, Synthesis and $Eu^{3+}$ luminescence in new oxysilicates, $ALa_3Bi(SiO_4)_3O$ and $ALa_2Bi_2(SiO_4)_3O$ [$A$=Ca, Sr and Ba] with apatite-related structure, J. Solid State Chem. 178 (2005) 3284–3292.
[4] J.M.S. Skakle, C.L. Dickson, F.P. Glasser, The crystal structures of $CeSiO_4$ and $Ca_2Ce_8(SiO_4)_6O_2$, Powder Diffr. 15 (2000) 234–238.
[5] M. Takahashi, K. Uematsu, Zuo-Guang Ye, M. Sato, Single-crystal growth and structure determination of a new oxide apatite, $NaLa_9(GeO_4)_6O_2$, J. Solid State Chem. 139 (2) (1998) 304–309.
[6] J. Huang, A.W. Sleight, The apatite structure without an inversion center in a new bismuth calcium vanadium oxide: $BiCa_4V_3O_{13}$, J. Solid State Chem. 104 (1993) 52–58.
[7] T.J. White, D. ZhiLi, Structural derivation and crystal chemistry of apatites, Acta Crystallogr. B 59 (1) (2003) 1–16.
[8] S. Nakayama, T. Kageyama, H. Aono, Y. Sadaoka, Ionic conductivity of lanthanoid silicates, $La_{10}(SiO_4)_6O_3$ ($La$=La, Nd, Sm, Gd, Dy, Y, Ho, Er and Yb), J. Mater. Chem. 5 (11) (1995) 1801–1805.
[9] TOPAS V3: General Profile and Structure Analysis Software for Powder Diffraction Data, User's Manual, Bruker AXS, Karlsruhe, Germany, 2003.
[10] G. Engel, W. Götz, R. Eger, Über bismuthaltige silicatapatite. Ungewöhnliche oxidapatite, Z. Anorg. Allg .Chem. 449 (1979) 127–134.
[11] M. Higuchi, Y. Masubuchi, S. Nakayama, S. Kikkawa, K. Kodaira, Single crystal growth and oxide ion conductivity of apatite-type rare-earth silicates, Solid State Ionics 174 (2004) 73–80.
[12] A. Quintas, O. Majerus, D. Caurant, J.-L. Dussossoy, P. Vermaut, Crystallization of a rare earth-rich aluminoborosilicate glass with varying $CaO/Na_2O$ ratio, J. Am. Ceram. Soc. 90 (3) (2007) 712–719.
[13] B.S. Mithcell, An Introduction to Materials Engineering and Science for Chemical and Materials Engineers, Wiley-IEEE, New York, 2004, p. 62.
[14] T. Dordevic, S. Sutovic, J. Stojanovic, L. Karanovic, Sr, Ba and Cd arsenates with the apatite-type structure, Acta Cryst. C 64 (2008) i82–i86.
[15] E.I. Get'man, N.V. Yablochkova, S.N. Loboda, V.V. Prisedsky, V.P. Antonovich, N.A. Chivireva, Isomorphous substitution of europium for strontium in the structure of synthetic hydroxovanadate, J. Solid State Chem. 181 (2008) 2386–2392.
[16] R. Astala, L. Calderin, X. Yin, M.J. Stott, Ab initio simulation of Si-doped hydroxyapatite, Chem. Mater 18 (2) (2006) 413–422.
[17] D. Arcos, J. Rodriguez-Carvajal, M. Vallet-Regi, The effect of silicon incorporation on the hydroxylapatite structure. A neutron diffraction study, J. Solid State Sci. 6 (2004) 987–994.
[18] Y. Otsuka, S. Fujihara, Transparent and luminescent thin films of partially substituted $La_{10}(SiO_4)_6O_3$:$Eu^{3+}$ apatite-type silicates, J. Electrochem. Soc. 154 (10) (2007) j335–j340.
[19] M. D'Apuzzo, A. Aronne, S. Esposito, P. Pernice, Sol-gel synthesis of humidity-sensitive $P_2O_5$-$SiO_2$ amorphous films, J. Sol–Gel Sci. Tech. 17 (2000) 247–254.
[20] R.H. Stolen, G.E. Walrafen, Water and its relation to broken bond defects in fused silica, J. Chem. Phys. 64 (1976) 2623–2631.
[21] W. Peng-Fei, D. Shi-Jin, Z. Wei, Z. Jian-Yun, W. Ji-Tao, L.W. Wei, FTIR Characterization of fluorine doped silicon dioxide thin films deposited by plasma enhanced chemical vapor deposition, Chin. Phys. Lett. 17 (2000) 912–914.
[22] W.A. Pliskin, in: H.R. Huff, R.R. Burgess (Eds.), Semiconductor Silicon, Electrochemical Society, Priceton, NJ, 1973, p. 506.
[23] Y.I. Ryskin, The vibrations of protons in minerals: hydroxyl, water and ammonium, in: V.C. Farmer (Ed.), Infrared Spectra of Minerals, Mineralogical Society, London, 1974, pp. 137–181 (Monograph No. 4).
[24] M. Alkan, C. Hopa, Z. Yilmaz, H. Güler, The effect of alkali concentration and solid/liquid ratio on the hydrothermal synthesis of zeolite NaA from natural kaolinite, Microporous Mesoporous Mater. 86 (2005) 176–184.
[25] E. Kendrick, D. Headspith, A. Orera, D.C. Apperley, R.I. Smith, M.G. Francesconi, P.R. Slater, An investigation of the high temperature reaction between the apatite oxide ion conductor $La_{9.33}Si_6O_{26}$ and $NH_3$, J. Mater. Chem. 19 (2009) 749–754.
[26] W.E. Morgan, W.J. Stec, J.R. Van Wezer, Inner-orbital binding-energy shifts of antimony and bismuth compounds, Inorg. Chem. 12 (1973) 953–955.
[27] J.T. Kloprogge, L.V. Duong, B.J. Wood, R.L. Frost, XPS study of the major minerals in bauxite: gibbsite, bayerite and (pseudo-) boehmite, J. Colloid Interface Sci. 296 (2006) 572–576.
[28] P. H .J. Mercier, Y. Le Page, P.S. Whitfield, L.D. Mitchell, I.J. Davidson, T.J. White, Geometrical parameterization of the crystal chemistry of $P6_3$/m apatites: comparison with experimental data an ab initio results, Acta Cryst. B 61 (2005) 635–655.
[29] I. Rosales, E. Orozco, L. Bucio, M.E. Fuentes, L. Fuentes, A synchrotron study of $Na_{2.27}$ $Ho_{7.73}$ $(SiO_4)_6$ $O_{0.72}$,, Acta Cryst. E 65 (5) (2009) i33-sup6.
[30] D. Nyfeler, T. Armbruster, Silanol groups in minerals and inorganic compounds, Am. Mineral. 83 (1998) 119–125.
[31] M. Healey, M.T. Weller, A.R. Genge, Synthesis and structure of NaZnSiO3OH, a new chiral zincosilicate framework material, Inorg. Chem. 38 (1999) 455–458.
[32] P. Gillespie, G. Gang Wu, M. Sayer, M.J. Stott, Si complexes in calcium phosphate biomaterials, J Mater. Sci: Mater. Med. 21 (2010) 99–108.